A Simple Wide-Band On-Chip Inductor Model for Silicon-Based RF IC's

Joonho Gil
Department of Electrical Engineering & Computer Science,
Korea Advanced Institute of Science and Technology,
373-1, Guseong-dong, Yuseong-gu, Daejeon, 305-701, Korea
e-mail: jgil@kaist.ac.kr

Hyungcheol Shin
School of Electrical Engineering,
Seoul National University, San 56-1, Shilim-dong,
Gwanak-gu, Seoul 151-742, Korea
e-mail: hcshin@ee.kaist.ac.kr

***Abstract*—In this paper, we developed a simple wide-band inductor model that contains lateral substrate resistance and capacitance to model the decrease in the series resistance at high frequencies related to lateral coupling through the silicon substrate. The model accurately predicts the equivalent series resistance and inductance over a wide-frequency range. Since it has frequency-independent elements, the proposed model can be easily integrated in SPICE-compatible simulators. The proposed model has been verified with measured results of inductors fabricated in a 0.18-μm 6-metal CMOS process. We also demonstrate the validity of the proposed model for shielded inductors. The proposed model shows excellent agreement with measured data over the whole frequency range.**

Keywords-inductor, inductor model, series resistance, substrate modeling, wide-band, substrate resistance, substrate capacitance

I. INTRODUCTION

Since advances in CMOS technology allowed the integration of RF circuits, low-frequency analog circuits, and digital baseband circuits [1], [2], it has been anticipated that a complex CMOS RF system on a chip (RF SoC) could be realized in the near future. In CMOS RF SoCs, numerous inductors are used. The inductor is a critical component for implementing RF circuits such as RF amplifiers, mixers, voltage-controlled oscillators, and impedance matching circuits. One of the most important issues related to on-chip inductors is accurate modeling suitable for circuit simulation. With an accurate model of an on-chip inductor, there are many advantages such as reduced turn-around-time, reduced design cost, and faster time-to-market. However, the lack of an accurate model for on-chip inductors presents one of the most challenging problems for silicon-based RF IC designers [1].

Many researchers have reported the modeling of inductors on a silicon substrate [3]-[11]. To include the effect of increase in series resistance (R_s) with frequency into the model, frequency dependent series resistance has been used in [5]-[7]. However, frequency dependent elements are difficult to implement in time domain simulators such as SPICE [8]. More recently, to overcome this restriction, models using only frequency independent elements have been reported [8]-[11]. However, the models in [8] and [9] could not predict the drop-down characteristics of R_s at higher frequency. While the model in [10] which has been constructed by a two-pi equivalent circuit could predict the drop-down characteristics,

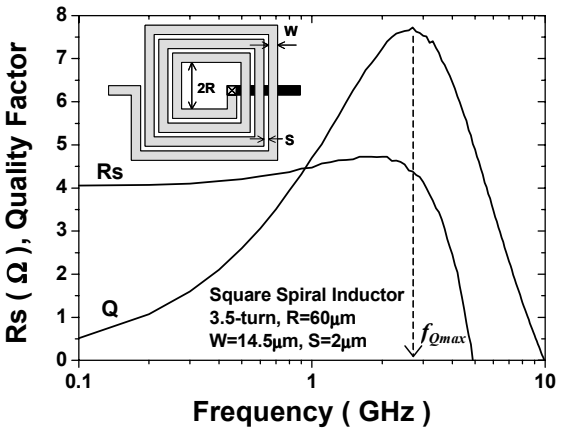

Fig. 1. Measured series resistance and quality factor for a 3.5-turn square spiral inductor. Insert shows the inductor layout.

it is somewhat complicated and has a large number of elements, which leads to greater time consumption in the circuit simulation. The distributed modeling approach on a segment-by-segment base to be applicable for both differential and common-mode excitations was used in [11]. The model of one segment is similar to the classical lumped model, and it has the lateral RC-coupling in the substrate. However, to take the frequency dependency of the series resistance and inductance into account, further dissection of inductor segments in parallel filaments is needed [11]. Thus, the resulting distributed model has large complexity even with some reductions (e.g., neglecting high-frequency effects of nonadjacent segments [11]).

In this paper, we propose a simple wide-band inductor model that has both drop-down characteristics and increase characteristics in R_s as a function of frequency. The proposed inductor model shows high accuracy over the entire frequency range by taking the coupling through the silicon substrate into account to model the decrease in R_s at high frequency. In the latter part of this paper, modeling results for shielded inductors are also presented.

II. A NEW INDUCTOR MODEL

Fig. 1 shows the measured series resistance (R_s) and quality factor (Q) of a 3.5-turn square spiral inductor. The equivalent

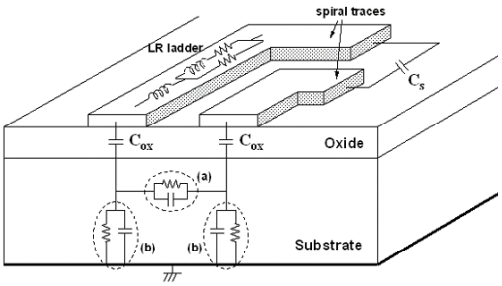

Fig. 2. Simplified illustration of the substrate network: (a) substrate lateral coupling resistance and capacitance and (b) substrate resistance and capacitance to ground.

series resistance $R_s(f)$ and series inductance $L_s(f)$ were extracted from Y_{21}:

$$R_s(f) + j\omega L_s(f) = -1/Y_{21}. \quad (1)$$

And the quality factor was evaluated by

$$Q = -Im(Y_{11})/Re(Y_{11}). \quad (2)$$

As the frequency increases, R_s increases mainly due to both skin and proximity effects. At the frequency reaching the maximum Q, R_s starts to decrease rapidly. Since the frequency of the maximum Q is generally set as the circuit operating frequency to utilize the highest performance of inductor, any decrease in R_s should be modeled accurately. We believe that the decrease is caused by coupling through the silicon substrate.

It was reported that a parallel combination of resistance and capacitance should be included in the modeling of two metal strips on a silicon substrate because the coupling mechanisms through the silicon substrate are resistive coupling dominant at low frequency and capacitive coupling dominant at high frequency [12]. In this manner, an on-chip inductor on a silicon substrate can be treated as a collection of metal strips with substrate coupling. As depicted in Fig. 2, the adjacent two metal strips have signal coupling at the silicon substrate via the oxide capacitance. Also, it is expected that all metal strips couple laterally to each other through the substrate. The substrate resistance and capacitance to ground ((b) in Fig. 2) have already been accounted for in many previously reported models, but the substrate lateral coupling resistance and capacitance ((a) in Fig. 2) have thus for far not been addressed, excluding the distributed models in [11]. Hence, to represent the lateral substrate coupling, R_{sub} and C_{sub} are introduced in our proposed model, as shown in Fig. 3. Contrary to the distributed model [11] and the two-cell model [10], the proposed model is constructed with a simple single-cell. A parallel combination of R_{sub} and C_{sub} is placed in the silicon substrate, similar to the equivalent circuit model for substrate coupling [12], [13] and on-chip interconnects [14]. C_{ox} represents the oxide capacitance between the inductor and the substrate. R_{si} and C_{si} are the substrate resistance and capacitance to ground, respectively. The series capacitance (C_s) models the capacitive coupling between input and output ports

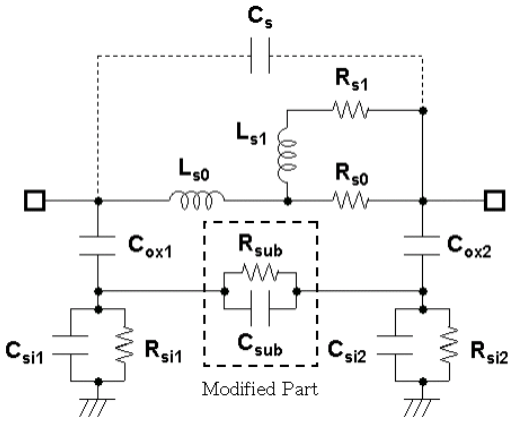

Fig. 3. Proposed inductor model with R_{sub} and C_{sub} to model substrate effects.

of the inductor. Since there is another capacitive coupling through the oxide capacitance (C_{ox}) and the substrate capacitance (C_{sub}) in the proposed model, the effect of C_s is redundant. Therefore, C_s is neglected in this paper. Moreover, the LR ladder circuit formed by L_{s1} and R_{s1} in parallel to R_{s0} [8], [10] is used to capture the increase in the series resistance due to both skin and proximity effects. Since all elements in the proposed model are frequency independent, the proposed model can be easily integrated in SPICE-compatible simulators.

III. Model Verification

In order to verify the accuracy of the proposed model, square spiral inductors with various geometrical configurations were fabricated using 0.18-μm 6-metal CMOS technology. The substrate resistivity is about 10 Ω-cm, the spiral metal thickness is 2 μm, and the oxide thickness between the spiral and the substrate is about 7.5 μm. The substrate contacts are placed 50 μm away from the inductor. Two-port S-parameters were measured using an Agilent 8510C network analyzer and RF probes. To characterize the intrinsic inductor, the pad parasitics were de-embedded from the measurement using an open pad structure. To isolate the pad from the substrate and to minimize substrate coupling effects by the probing pad, a grounded metal-1 shield was implemented under the probing pad [15]. Model parameters were extracted by fitting the proposed model to the measured Y-parameters using HSPICE optimization routines. To assess the model validity, the equivalent series resistance $R_s(f)$, series inductance $L_s(f)$, and the quality factor were evaluated by (1) and (2).

Fig. 4 shows $R_s(f)$ and $L_s(f)$ curves for six test structures with varying number of turns. As the measurement curves show, the series resistance increases with frequency at first and drops down at higher frequency. The decrease in $R_s(f)$ is caused by the lateral substrate coupling among inductor metal strips. As shown in Fig. 4(a), the model without R_{sub} and C_{sub} could predict only the increase in R_s but could not model the decrease in R_s at higher frequency. Also, as shown in Fig. 4(b), the proposed model predicts the change in inductance as a function of frequency, but the model without R_{sub} and C_{sub} does

0-7803-7826-1/03/$17.00 © 2003 IEEE

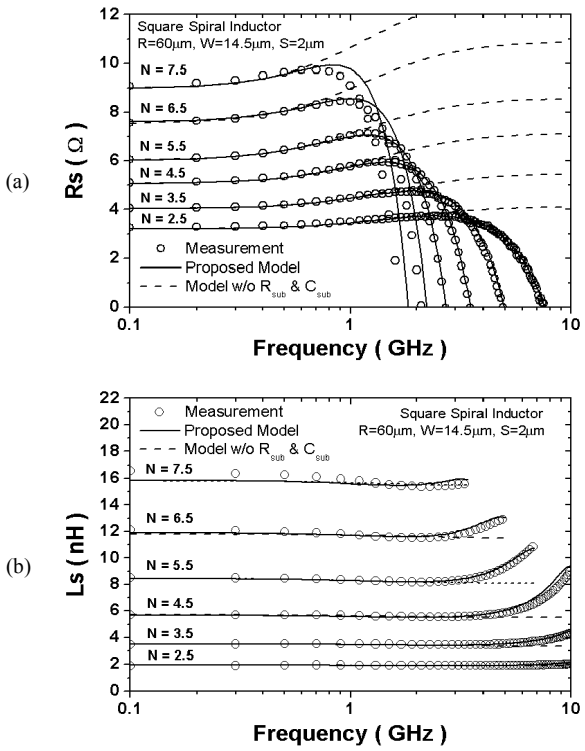

Fig. 4. Comparison between the measurement and the model. (a) Series resistance and (b) series inductance as a function of frequency and the number of turns.

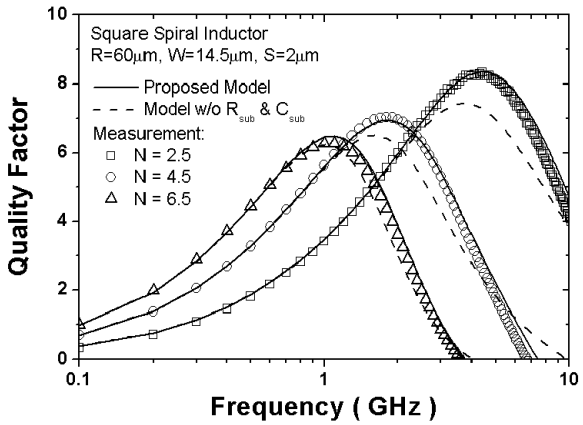

Fig. 5. Quality factor comparison of the proposed model with the model without R_{sub} and C_{sub}.

not. The model without R_{sub} and C_{sub} significantly overestimates R_s and underestimates L_s at high frequency, which introduces large error in circuit simulations such as transient analysis [2], [10]. As the number of turns increases, the substrate coupling between the metal strips becomes larger because C_{ox} and C_{sub} are larger (see Table I). Therefore, $R_s(f)$ drops at lower frequency for inductors with a larger number of turns. A quality factor comparison of the proposed model with the model without R_{sub} and C_{sub} is shown in Fig. 5. A significant improvement in prediction is observed at the frequency near the peak Q.

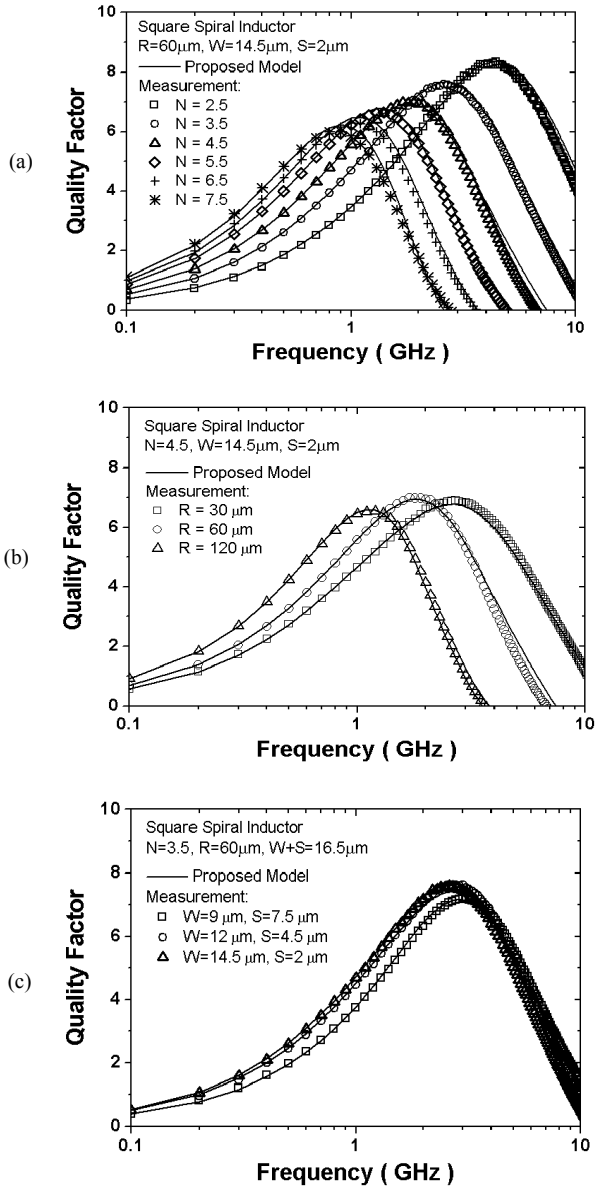

Fig. 6. Measured and modeled quality factor of (a) various numbers of turns, (b) various inner radii, and (c) various metal widths and spacing.

Fig. 6 verifies the quality factor for different numbers of turns, inner radii, and metal widths and spacing. The proposed model matched accurately with the measurements over the whole frequency range of interest. Also, we obtained excellent agreement in the peak Q, the frequency at the peak Q, and the self-resonance frequency. The proposed model shows excellent scalability and wide-band accuracy. Wide-band models would be useful for broadband circuit design.

The model parameters of inductors with different geometries are summarized in Table I. As the number of turns (N) or the inner radius (R) increases, both inductance and resistance parameters increase simultaneously. In general, C_{ox} and C_{si} are proportional to the area of the inductor and R_{si} is inversely proportional to the area occupied by the inductor [5]. The model parameters in Table I also exhibit the same trends.

TABLE I. SUMMARY OF MODEL PARAMETERS FOR INDUCTORS WITH DIFFERENT GEOMETRIES

Dimension (N×R×W×S)	Model Parameters Fit to Measurement												
	L_{s0} (nH)	L_{s1} (nH)	R_{s0} (Ω)	R_{s1} (Ω)	C_{ox1} (fF)	C_{ox2} (fF)	R_{si1} (Ω)	R_{si2} (Ω)	C_{si1} (fF)	C_{si2} (fF)	R_{sub} (Ω)	C_{sub} (fF)
2.5×60×14.5×2	1.87	1.84	4.12	14.20	91.8	89.5	372.1	369.4	24.1	24.0	1.6K	94.8
3.5×60×14.5×2	3.36	2.19	5.49	15.19	120.2	115.9	282.4	276.1	33.4	33.3	2.8K	101.5
4.5×60×14.5×2	5.42	2.92	7.15	17.27	161.5	152.1	238.2	232.1	49.7	47.8	5.7K	155.8
5.5×60×14.5×2	8.09	4.01	8.58	20.15	196.2	188.5	186.3	184.3	52.5	51.9	8.4K	199.1
6.5×60×14.5×2	11.49	4.92	10.71	26.13	236.8	228.4	147.6	142.8	63.2	61.9	18.6K	291.7
7.5×60×14.5×2	15.43	5.92	12.21	35.11	281.7	272.8	100.8	99.5	75.6	72.8	30.1K	670.5
4.5×30×14.5×2	3.02	1.19	6.68	7.58	120.6	113.6	292.9	288.0	34.1	33.0	1.0K	71.5
4.5×120×14.5×2	10.92	7.72	9.19	45.02	257.0	250.9	138.1	127.6	74.8	73.3	14.2K	402.1
3.5×60×9×7.5	3.49	1.43	7.24	26.30	88.3	85.1	360.1	358.8	11.1	10.5	8.4K	60.4
3.5×60×12×4.5	3.44	2.02	6.05	16.12	104.9	97.8	309.1	307.9	21.6	19.9	6.4K	73.1

* N: number of turns, R: inner radius (μm), W: metal width (μm), S: spacing (μm).

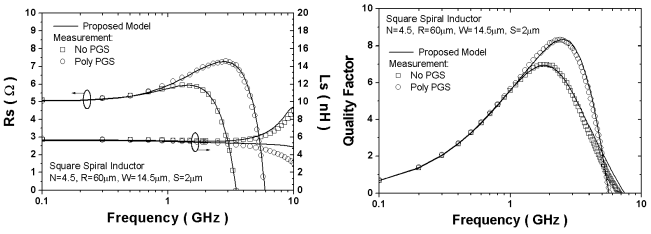

(a) (b)

Fig. 7. Modeling results for shielded inductor. (a) Series resistance and inductance. (b) Quality factor.

Using an extrapolation to a wide range of geometries with the model parameters, a complete inductor model library can be constructed. In circuit applications, this allows for designing an inductor with optimized circuit performance. Because model parameters were extracted by fitting, the values will not be valid for different processes. However it is possible for the model parameters to be reconstructed by multiplying the scaling factor obtained from the process parameters. For example, if the oxide thickness decreases, the oxide capacitances (C_{ox1}, C_{ox2}) will increase by the same ratio. Consequently, based on the model parameters listed in Table I, it is anticipated that a good fit can be achieved for different processes by scaling the model parameters according to the changes of the process parameters.

Patterned ground shields (PGS) are widely used to improve the performance of inductors by decoupling the inductor from the substrate [16]. To investigate the validity of the proposed model for a PGS inductor, a PGS inductor was measured and modeled. The silicided polysilicon ground shield has 2.5 μm slot width and 5 μm slot pitch. Fig. 7 shows results of the modeling for the PGS inductor using the proposed model. R_s of the PGS inductor decreases at a much higher frequency compared with the unshielded inductor due to the reduced substrate effect. The proposed model shows excellent agreement with the measurements in the quality factor as well as R_s and L_s.

IV. CONCLUSION

A simple wide-band model for on-chip inductors on a silicon substrate is presented. The proposed model contains a parallel combination of resistance and capacitance in the substrate to model lateral substrate coupling. Verification with measurement data from various structures and shielded patterns demonstrates the validity of the proposed model. The model shows excellent agreement with measured data over the entire frequency range of interest. Our new model can be easily implemented in SPICE-compatible simulators to improve accuracy in circuit simulation.

ACKNOWLEDGMENT

This work was supported by KOSEF through the MICROS center at KAIST and Hynix Semiconductor Inc. The authors would like to thank Prof. Kwyro Lee for valuable comments.

REFERENCES

[1] M. Je, I. Kwon, H. Shin, and K. Lee, "MOSFET modeling and parameter extraction for RF-IC's," a book chapter in CMOS RF Modeling, Characterization and Applications, World Scientific, pp. 67-120, 2002.

[2] D. Leenaerts, G. Gielen, and R. A. Rutenbar, "CAD solutions and outstanding for mixed-signal and RF IC design," IEEE/ACM Int. Conf. Computer Aided Design, pp. 270-277, 2001.

[3] J. R. Long and M. A. Copeland, "The modeling, characterization, and design of monolithic inductors for silicon RF IC's," IEEE J. Solid-State Circuits, vol. 32, pp. 357-368, 1997.

[4] A. M. Niknejad and R. G. Meyer, "Analysis, design, and optimization of spiral inductors and transformers for Si RF IC's," IEEE J. Solid-State Circuits, vol. 33, pp. 1470-1481, 1998.

[5] C. P. Yue and S. S. Wong, "Physical modeling of spiral inductors on silicon," IEEE Trans. Electron Devices, vol. 47, pp. 560-568, Mar. 2000.

[6] M. Park, et al., "Frequency-dependent series resistance of monolithic spiral inductors," IEEE Microwave and Guided Wave Letters, vol. 9, No. 12, pp. 514-516, Dec. 1999.

[7] W. B. Kuhn and N. M. Ibrahim, "Analysis of current crowding effects in multiturn spiral inductors," IEEE Trans. Microwave Theory and Techniques, vol. 49, pp. 31-38, Jan. 2001.

[8] T. Kamgaing, T. Myers, M. Petras, and M. Miller, "Modeling of frequency dependent losses in two-port and three-port inductors on silicon," IEEE MTT-S, pp. 153-156, 2002.

[9] C-J. Chao, S-C. Wong, C-J. Hsu, M-J. Chen, and L-Y. Leu, "Characterization and modeling of on-chip inductor substrate coupling effect," IEEE RF-ICs Symp., pp. 311-314, 2002.

[10] Y. Cao, et al., "Frequency-independent equivalent circuit model for on-chip spiral inductors," IEEE Custom Integrated Circuits Conf., pp. 217-220, 2002.

[11] G. Grau, et al., "A current-folded up-conversion mixer and VCO with center-tapped inductor in a SiGe-HBT technology for 5-GHz wireless LAN applications," IEEE J. Solid-state Circuits, vol.35, no.9, pp. 1345-1352, Sep. 2000.

[12] W. Jin, et al., "Silicon substrate coupling noise modeling, analysis, and experimental verification for mixed signal integrated circuit design," IEEE MTT-S, pp. 1727-1730, 2001.

[13] A. Adan, M. Fukumi, K. Higashi, T. Suyama, M. Miyamoto, and M. Hayashi, "Electromagnetic coupling effects in RFCMOS circuits," IEEE Radio Frequency Integrated Circuits Symposium, pp 293-296, 2002.

[14] J. Zheng, Y-C. Hahm, V. K. Tripathi, and A. Weisshaar, "CAD-oriented equivalent-circuit modeling of on-chip interconnects on lossy silicon substrate," IEEE Trans. Microwave Theory and Techniques, vol. 48, No. 9, pp. 1443-1451, Sep. 2000.

[15] A. Aktas and M. Ismail, "Pad de-embedding in RF CMOS," IEEE Circuits and Devices Magazine, vol. 17 Issue 3, pp. 8-11, May 2001.

[16] C. P. Yue and S. S. Wong, "On-chip spiral inductors with patterned ground shields for Si-based RF IC's," IEEE J. Solid-State Circuits, vol. 33, pp. 743-752, 1998.

